SPANDIDOS PUBLICATIONS

ONCOLOGY LETTERS 15: 4201-4206, 2018

Integrin αVβ$_3$-targeted SPECT/CT for the assessment of Bevacizumab therapy in orthotopic lung cancer xenografts

BIN CHEN*, WENQI ZHANG*, BIN JI, QINGJIE MA, DANDAN LI and SHI GAO

Department of Nuclear Medicine, China-Japan Union Hospital of Jilin University, Erdao, Changchun 130033, P.R. China

Received January 4, 2017; Accepted December 4, 2017

DOI: 10.3892/ol.2018.7901

Abstract. The present study aimed to determine the utility of ^{99m}Tc-3PRGD$_2$ single photon emission computed tomography (SPECT)/computed tomography (CT) for the non-invasive monitoring of the response of integrin $\alpha_v\beta_3$ expression to anti-angiogenic treatment with bevacizumab. Bevacizumab or vehicle therapy was performed in athymic nu/nu mice bearing A549 lung tumors (moderately high integrin $\alpha_v\beta_3$ expression) or PC-3 prostate tumors (low integrin $\alpha_v\beta_3$ expression) at a dose of 1 mg twice a week. The average tumor volume was 180±90 mm^3 the day prior to baseline SPECT/CT. Longitudinal ^{99m}Tc-3PRGD$_2$ SPECT/CT imaging was performed at baseline (-1 day) and at days 5 and 15. Tumors were harvested at all imaging time points for histopathological analysis with hematoxylin and eosin (H&E) and immunohistochemistry staining. Results revealed a significant difference in tumor volume between vehicle- and bevacizumab-treated groups at 5 and 15 days following the start of treatment in the A549 lung model (P<0.05). At 5 days after the start of therapy, the percent injected dose per gram of tissue (%ID/g) and tumor-to-muscle ratio for bevacizumab-treated A549 declined persistently (P<0.05). However, for the vehicle-treated A549 model, the %ID and %ID/g value increased 5 days after the start of treatment (P<0.05). For the PC-3 model, slow-growing tumors and low tumor uptake was observed throughout the study. Alterations in tumor vasculature were confirmed by histopathological H&E analysis and immunohistochemistry. In conclusion, longitudinal imaging using ^{99m}Tc-3PRGD$_2$ SPECT/CT may be a useful tool for monitoring the anti-angiogenic effect of bevacizumab therapy.

Correspondence to: Professor Dandan Li or Professor Shi Gao, Department of Nuclear Medicine, China-Japan Union Hospital of Jilin University, 126 Xiantai Street, Erdao, Changchun 130033, P.R. China
E-mail: 232353666@qq.com
E-mail: gaoshi@jlu.edu.cn

*Contributed equally

Key words: ^{99m}Tc-3PRGD2 single photon emission computed tomography/computed tomography, lung cancer, bevacizumab

Introduction

Inhibition of angiogenesis is a promising strategy for breast and lung cancer therapy (1,2). It has been demonstrated that combined therapy with angiogenesis inhibitors may significantly enhance the treatment effect and extend survival in breast and lung cancer patients (3,4). However, inhibitors of angiogenesis tend to be expensive and are not effective in a proportion of cancer patients (5). In addition, the tumor volume changes are much slower than blood supply inhibition. Conventional tools [X-ray and computed tomography (CT)] rely on tumor volume change to evaluate the effect of tumor, which is not suitable for antiangiogenic drugs (6). Therefore, it is critical that a reliable tool is identified to monitor and assess the treatment effect of inhibiting angiogenesis therapy.

Imaging tools have been used to monitor cancer therapy for decades (7,8). In this area, nuclear medicine imaging techniques are promising. ^{99m}Tc-3PRGD$_2$ single-photon emission computed tomography (SPECT)/CT has been developed as an imaging modality for evaluating tumor vascular status (9,10). ^{99m}Tc-3PRGD$_2$ is a radiolabeled dimeric arginylglycylaspartic acid (RGD) peptide that is being investigated for measurement of the expression of integrin $\alpha_v\beta_3$ (11). Integrin $\alpha_v\beta_3$ is widely distributed in newly generated vessels. Additionally, this subtype of integrin has been documented as being associated with tumor angiogenesis and metastasis (12). Therefore, the degree of expression of integrin $\alpha_v\beta_3$ may reflect the status of tumor angiogenesis.

Bevacizumab is a recombinant humanized monoclonal antibody that blocks angiogenesis by inhibiting vascular endothelial growth factor-A (VEGF-A); it has been used to treat breast and lung cancer since 2004, and has shown promising therapeutic results (3). The present study determined the utility of imaging the uptake of ^{99m}Tc-3PRGD$_2$ by tumors as a biomarker for anti-angiogenic treatment with bevacizumab in a lung cancer A549 cell xenograft model, which has high-to-moderate vessel density and exhibits integrin $\alpha_v\beta_3$ expression, and a PC-3 prostate cancer model, which has low vessel density and also exhibits integrin $\alpha_v\beta_3$ expression. Following the present study, how changes in tumor uptake of ^{99m}Tc-3PRGD$_2$ affect the tumor response to antiangiogenic treatment can be better understood before it can be used clinically to monitor investigational therapy.

Materials and methods

Animal models and treatment protocol. All animal experiments were performed in accordance with the protocol approved by

the Institutional Animal Care and Use Committee at Jilin University (Changchun, China). The A549 and PC-3 cell lines were obtained from the American Type Culture Collection (Manassas, VA, USA). These cells were cultured in F-12 medium (Gibco, Life Technologies, Grand Island, NY, USA) supplemented with 10% fetal bovine serum (Gibco; Thermo Fisher Scientific, Inc., Waltham, MA, USA) and 1% penicillin and streptomycin (Gibco; Thermo Fisher Scientific, Inc.) solution at 37˚C in a humidified atmosphere of 5% CO_2. Cells were grown as a monolayer and were harvested or passaged when they reached 90% confluence to maintain exponential growth. A total of 30 male Athymic nu/nu mice were obtained from the Department of Experimental Animals (Peking University) at 4-5 weeks of age. Mice were housed under standard laboratory conditions (temperature, 20-24˚C; relative humidity, 50-60%, 12/12 h light/dark cycle) and had food and water available *ad libitum*. Each mouse was implanted subcutaneously near the shoulder with 5x10^6 cells. At 4 weeks after inoculation with A549 and PC-3 cells, the mice were divided into three groups, with 9 or 10 mice in each group. All the groups were size-matched, with an average tumor volume of 180±90 mm^3 1 day before baseline SPECT/CT imaging. Vehicle (0.15% hydroxypropylmethyl cellulose, 2% ethanol, 5% Tween 80, 20% PEG 400 and 73% saline) or bevacizumab (Genentech, San Francisco, CA, USA) was injected intraperitoneally. The treatment protocol of each group was: A549 Bevacizumab group (A549 model, n=10), 1 mg bevacizumab twice a week from day 0 after baseline imaging; A549 Vehicle group (A549 model, n=10), vehicle with a dose of 1 mg twice a week from day 0 after baseline imaging; and PC-3 Bevacizumab group (PC-3 model, n=9), 1 mg bevacizumab twice a week from day 0 after baseline imaging.

Preparation of ^{99m}Tc-3PRGD$_2$ and small animal SPECT/CT. Na^{99m}TcO$_4$ was obtained from a commercial ^{99}Mo-^{99m}Tc generator (Beijing Atom High Tech Co., Ltd., Beijing, China). The kit for preparation of ^{99m}Tc-3PRGD$_2$ was formulated by containing 20 μg/ml of HYNIC-3P$_4$-RGD$_2$, 5 mg of TPPTS, 6.5 mg of tricine, 40 mg of mannitol, 38.5 mg of disodium succinate hexahydrate and 12.7 mg of succinic acid. Then 1 ml of Na^{99m}TcO$_4$ solution (1110-1850 MBq) in saline was added to each kit vial followed by 20 min incubation at 100˚C (11,13). The radiochemical purity of the prepared ^{99m}Tc-3PRGD$_2$ was >90%. Helical CT and SPECT scans of rats were obtained using a SPECT/CT system (NanoScan; Mediso Medical Imaging Systems, Budapest, Hungary). Longitudinal SPECT/CT imaging was performed at baseline (-1), 5, and 15 days after treatment initiation. At 1 h prior to SPECT/CT imaging, 37.0-44.4 MBq ^{99m}Tc-3P-RGD$_2$ in 0.1-0.2 ml of saline was administered intravenously via the lateral tail vein. Animals were anesthetized with 3% isoflurane inhalation, which was maintained at 1.5% for the duration of scanning, and then placed in a prone position in an air-warmed chamber. For radioactivity quantification, the regions of interest were drawn manually to cover the entire tumor, based on a transverse view of the CT image. For tumor delineation with SPECT, a threshold of ≥50% of the maximum pixel value on the SPECT image was chosen. Tumor volume and radioactivity counts were generated using NanoScan Image Processing software (version 3.306; PMOD Technologies LLC, Zürich, Switzerland) and the amount of radioactivity in each tumor was calculated. The tumor uptake of ^{99m}Tc-3PRGD$_2$ was expressed as the percent-injected dose (%ID) and %ID/g. Reference regions of interest were drawn over muscle as background radioactivity for tumor-to-muscle (T/M) ratio calculations.

Tumor immunostaining. Immunofluorescence staining was performed to determine the location and expression of integrin $\alpha_v\beta_3$. Tumors were sectioned into two pieces for immunostaining and hematoxylin and eosin (H&E) staining. Once tumors were harvested, the tumor sections for immunostaining were immediately snap-frozen in optical cutting temperature solution (99% purity, Sigma-Aldrich; Merck KGaA, Darmstadt, Germany). Tumors were then cut into 5-mm sections. Following thorough drying at room temperature, slides were fixed with ice-cold acetone for 10 min, and air-dried for 20 min at room temperature. The sections were then blocked with 10% goat serum (Abcam, Cambridge, MA, USA) for 30 min at room temperature and then incubated with rat anti-integrin β_3 antibody (1:100; cat. no. 181720; BD Biosciences, Franklin Lakes, NJ, USA) and rat anti-CD31 antibody (1:100; cat. no. 551262; BD Biosciences) for 1 h at room temperature. The β_3 antibody was chosen to represent $\alpha_v\beta_3$ as the only other integrin with an $\alpha\beta_3$ subunit besides $\alpha_v\beta_3$ is expressed on platelets. The majority of β_3 in the tumor sections is likely to be in the vasculature and tumor cells. After incubating with Cy3-conjugated goat anti-rat (1:100; cat. no. 115-165-003; Jackson ImmunoResearch Europe Ltd., Newmarket, UK) and fluoresceinisothiocyanate-conjugated goat anti-rat secondary antibodies (1:100; cat. no. 115-095-003; Jackson ImmunoResearch Europe Ltd.) at room temperature (25˚C) for 4 h, the sections were washed with PBS. Fluorescence was visualized with a Nikon fluorescence microscope at x200 magnification (Nikon Eclipse E600; Nikon Corporation, Tokyo, Japan).

H&E staining. Histopathological analysis was performed by H&E staining of tumors according to previously published methods (14). Briefly, all the tissues were fixed in 10% neutral buffered formalin at room temperature (25˚C) for 4 h. Tissues were embedded in paraffin and 4-mm sections were deparaffinized and rehydrated using a graded alcohol series. Sections were stained with H&E at room temperature (25˚C) for 20 min to evaluate the morphology and then examined under a light microscope. Aperio's Image Scope v10.1.3.2028 Viewer (Leica Mircosystems, GmbH, Wetzlar, Germany) was used to visualize the whole-slide digital scans and capture images in 30 fields of view for analysis.

Statistical analysis. All data were expressed as the mean ± standard error. Statistical analyses were performed by two-way analysis of variance followed by the Newman-Keuls test for multiple comparisons to compare treatment groups. $P<0.05$ was considered to indicate a statistically significant difference. A one-way analysis of variance and Newman-Keuls post-hoc test was performed to determine alterations over time. SPSS 19.0 software package (IBM Corp., Armonk, NY, USA) was used for linear and nonlinear regression analysis.

Results

Tumor volume in bevacizumab-treated tumor models. Fig. 1 depicts the tumor volumes for A549 Bevacizumab,

A549 Vehicle and PC-3 Bevacizumab groups. In the PC-3 Bevacizumab and A549 Vehicle group, the tumor volume increased at 5 and 15 days after therapy. The difference in tumor volume was not significantly different prior to and following treatment in the A549 Bevacizumab group (P>0.05).

Tumor uptake in bevacizumab-treated tumor models. Fig. 2 compared the %ID tumor uptake (Fig. 2A), %ID/g tumor uptake (Fig. 2B) and T/M ratios (Fig. 2C) of ^{99m}Tc-3PRGD$_2$ in the A549 Bevacizumab, A549 Vehicle and PC-3 Bevacizumab groups. For the PC-3 Bevacizumab group, a lower tumor uptake was observed throughout the study compared with the other 2 groups, and there was no significant alteration prior to and following bevacizumab therapy. After 5 and 15 days therapy, the %ID/g value for A549 Bevacizumab group declined. However, for the A549 Vehicle group, the %ID value increased 5 days after injection, but the %ID/g tumor uptake decreased after 5 and 15 days therapy as the weight of the tumor increased. For the A549 Bevacizumab and A549 Vehicle groups, the T/M ratio decreased 5 and 15 days after injection. Further SPECT/CT studies confirmed that bevacizumab-treated tumors have persistent tumor uptake decrease. Fig. 3 depicted SPECT/CT images for decreased uptake of ^{99m}Tc-3PRGD$_2$ of tumors in the A549 Bevacizumab group after treatment, increased uptake in the A549 Vehicle group, and low uptake of ^{99m}Tc-3PRGD$_2$ before and after treatment in the PC-3 Bevacizumab group.

Change in microvessel density (MVD) following bevacizumab treatment. Fig. 4 depicts selected histological slices (H&E stained) of tumor tissues from animals before and after 5 and 15 days of A549 Bevacizumab, A549 Vehicle and PC-3 Bevacizumab groups. The PC-3 model exhibited low MVD throughout the study. Prior to bevacizumab therapy, the MVD of the A549 model was moderately high. After 15 days therapy, the MVD of the A549 model was significantly lower than before therapy.

Change in integrin $\alpha_v\beta_3$ following bevacizumab treatment. Fig. 5 depicts overlay images of A549 and PC-3 tumor tissues after immunohistochemical staining for integrin β_3 and CD31 in A549 Bevacizumab, A549 Vehicle and PC-3 Bevacizumab groups. The PC-3 model exhibited low integrin β_3 levels. At 5 days after the start of therapy, the integrin β_3 level in the bevacizumab-treated models decreased. No evident alterations in the levels of CD31 were observed following bevacizumab-treatment. In the vehicle-treated model, the expression level of integrin β_3 was elevated. At 15 days after the start of therapy, the integrin β_3 and CD31 levels in the bevacizumab-treated models decreased. In the vehicle-treated model, tumor volume increased and integrin β3 and CD31 levels decreased, which may be due to the lack of neovascularization in the deep tumor tissue.

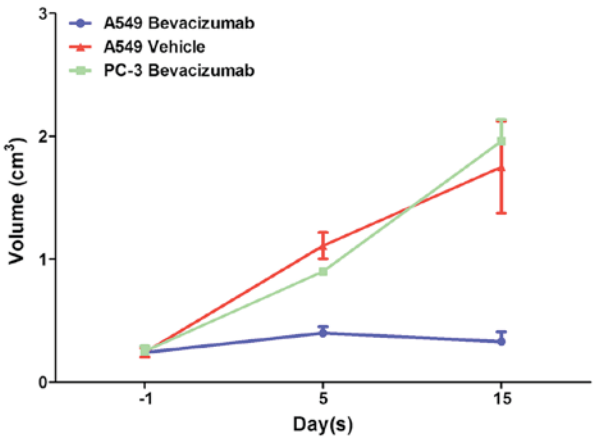

Figure 1. Comparison of tumor volumes between the A549 Bevacizumab (n=10), A549 Vehicle (n=10) and PC-3 Bevacizumab (n=9) groups in the mouse tumor model. Tumor volumes were determined by caliper measurements.

Discussion

Multiple growth factors, including VEGF and platelet-derived growth factor (PDGF) elevate integrin $\alpha_v\beta_3$ levels *in vitro* (15). Consequently, suppressing the expression or signaling of VEGF and PDGF receptors may decrease integrin $\alpha_v\beta_3$ levels. The target site of bevacizumab is VEGF and PDGF receptors. Therefore, integrin $\alpha_v\beta_3$ may be deemed to be a relevant biomarker for the evaluation of the biological effects that occur following bevacizumab therapy. Previous enhanced magnetic resonance imaging studies have indicated that, either in preclinical or clinical studies, a tumor vasculature system experiences alterations following bevacizumab therapy (16-18). In the present study, SPECT/CT was used to dynamically observe changes in ^{99m}Tc-3PRGD$_2$ uptake at two imaging time points, prior to and following dosing with bevacizumab in xenografts. At 5 days after the start of therapy, a significant decrease in the tumor uptake in the A549 model was observed. At 15 days after the start of therapy, the tumor volume in the A549 model mildly decreased. In comparison, the tumor volume in the PC-3 model and the vehicle-treated model increased. Additionally, the tumor uptake consistently increased in the vehicle-treated model. Therefore, ^{99m}Tc-3PRGD$_2$ SPECT/CT may be used in early therapy monitoring in bevacizumab treatment in the A549 model, but not in the PC-3 model.

The present study revealed that the degree of increase in %ID/g and T/M values were evident in the A549 model. Previous studies indicated that the treatment effect of bevacizumab was closely associated with MVD and integrin $\alpha_v\beta_3$ levels in different tumor types, which may explain differences with the present study (18). Compared with the PC-3 model, which had low MVD, the A549 model, with moderately high MVD, may express higher levels of integrin $\alpha_v\beta_3$. Further studies using models with poor integrin $\alpha_v\beta_3$ expression are required to investigate whether SPECT/CT could be used to rule out integrin $\alpha_v\beta_3$ expression non-invasively in an experimental and clinical setting.

MVD is the number of vessels per unit area of tumor tissue; it directly reflects the capability of formation of new tumor vessels. MVD is positively associated with tumor metastasis and proliferation, and can be used as an index for evaluating therapeutic effects of solid tumors (19,20). Through observing alterations in tumor microvessels via H&E staining, the present study demonstrated that the MVD of the bevacizumab treated model significantly decreased. The immunofluorescence

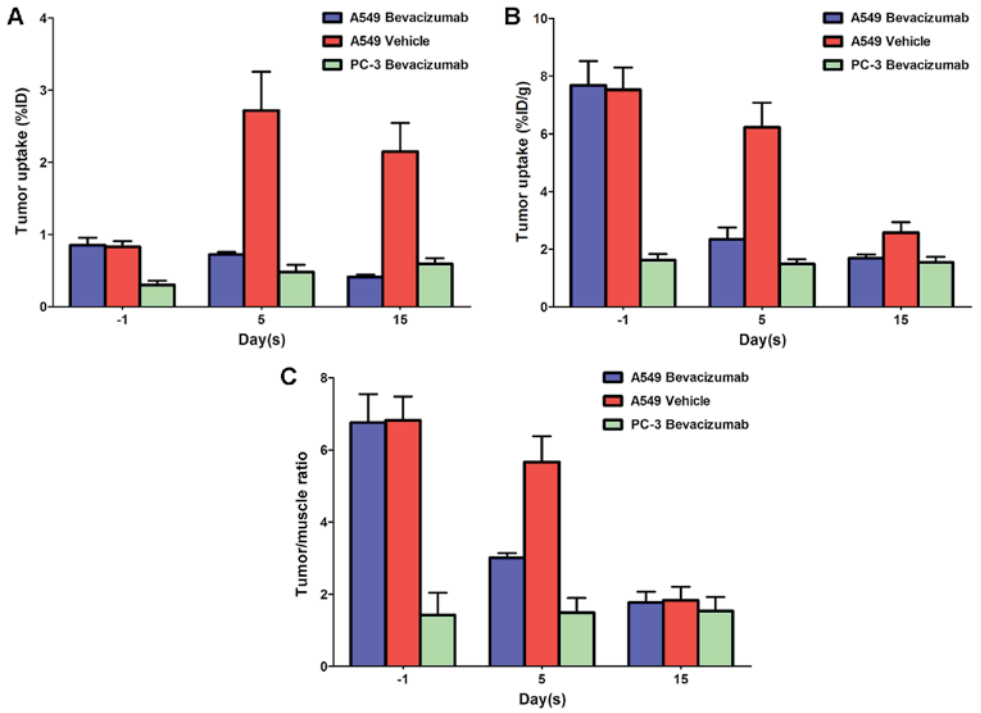

Figure 2. Comparison of the (A) %ID tumor uptake, (B) %ID/g tumor uptake and (C) T/M ratios in A549 Bevacizumab (n=10), A549 Vehicle (n=10) and PC-3 Bevacizumab (n=9) groups. Tumor uptake values and T/M ratios were calculated from SPECT/CT images of the mouse models. ID, injected dose; T/M, tumor-to-muscle; SPECT/CT, single photon emission computed tomography/computed tomography.

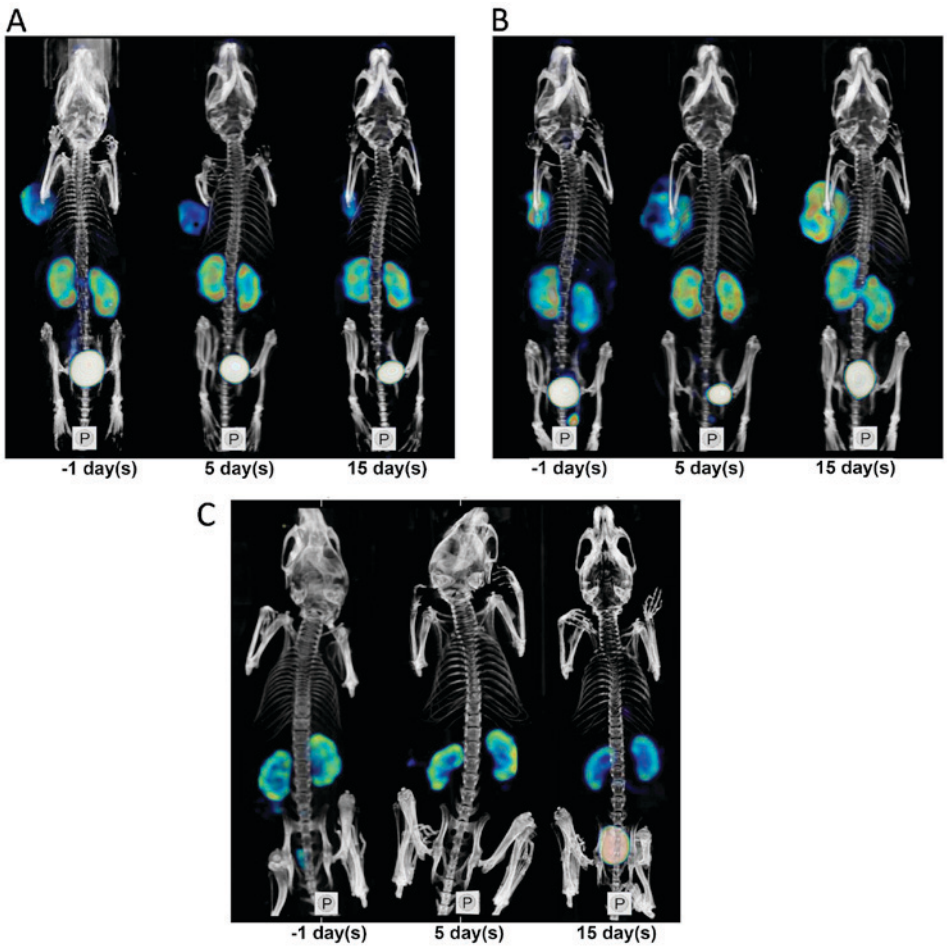

Figure 3. SPECT/CT images from (A) bevacizumab-treated and (B) vehicle-treated A549 tumor models and (C) bevacizumab-treated PC-3 tumor models. SPECT/CT images were obtained at baseline (-1), and at 5 and 15 days after initiation of bevacizumab therapy. SPECT/CT, single photon emission computed tomography/computed tomography.

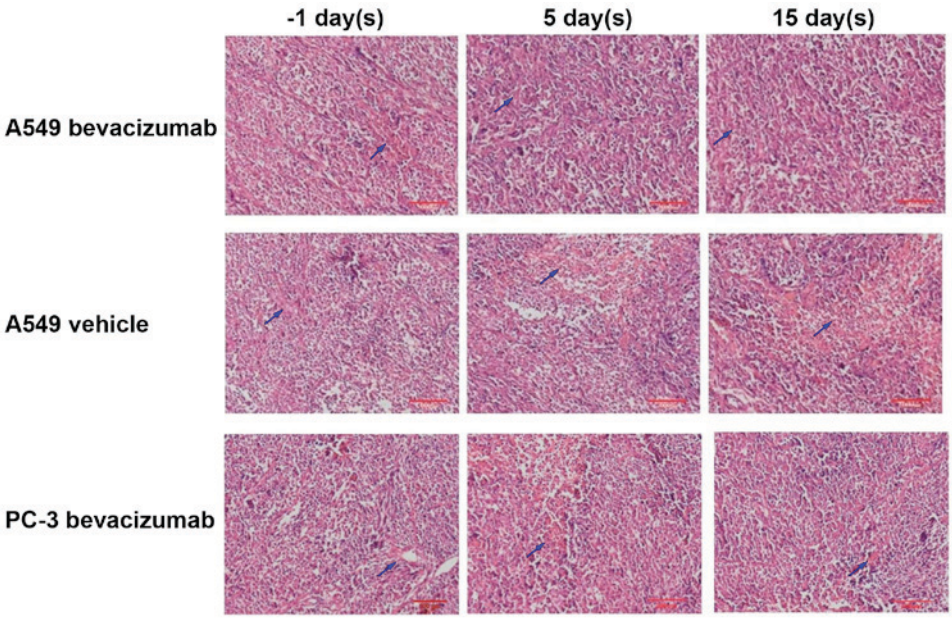

Figure 4. Histological slices of tumor tissues of A549 and PC-3 from animals at baseline (-1), and 5 and 15 days after initiation of bevacizumab therapy, illustrating alterations in vascular density.

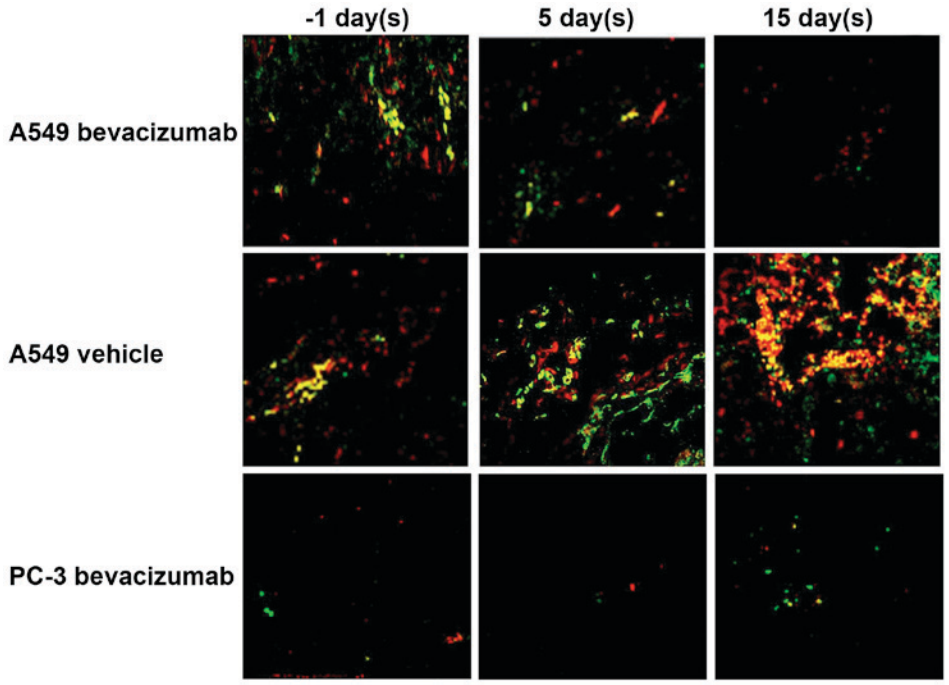

Figure 5. Images of A549 and PC-3 tumor tissues following immunohistochemical staining for integrin β_3 and CD31 in vehicle- and bevacizumab-treated groups to illustrate the alterations in integrin β_3 expression levels and blood vessel density during therapy. Tumor tissues were harvested at -1, 5 and 15 days after initiation of bevacizumab therapy. CD31 was used as the marker for tumor blood vessels (mature and newly formed), which was visualized with fluorescein isothiocyanate (green color). Integrin β_3 was visualized with cyanine 3 (red color). The yellow color in overlay images indicates the integrin β_3 expression on new blood vessels. Original magnification x200. CD31, cluster of differentiation 31.

staining results during therapy suggested that at 5 days after the start of therapy, a decrease of integrin $\alpha_v\beta_3$ on the surface of tumor cell was not evident, whereas the decrease of integrin $\alpha_v\beta_3$ within the new epithelial cells was. These results indicated the anti-angiogenic effect of bevacizumab and may explain the decrease of ^{99m}Tc-3PRGD$_2$ SPECT/CT uptake in tumors. ^{18}F-labeled peptides such as ^{18}F-fluciclatide and ^{18}F-FPPRGD$_2$ have been used to monitor the therapeutic effects of anti-angiogenic agents, including sunitinib, ZD4190 and functional paclitaxel (21-23). The results of the present study are in accordance with these previous studies. Considering the availability of pharmacokinetics, biodistribution, radiation dose and ^{9m}Tc-3PRGD$_2$, we hypothesize that ^{99m}Tc-3PRGD$_2$ SPECT/CT could be more cost-effective compared with the ^{18}F-labeled analogs. The T/M ratio of tumor RGD uptake was linearly associated with integrin $\alpha_v\beta_3$ and CD31 expression, as

previously reported (13). Quantitative analysis revealed that ^{99m}Tc-3PRGD$_2$ SPECT/CT was prominent in future clinical applications (24). However, to understand the association between T/M ratio and the treatment effects better, further research is required.

In conclusion, in the A549 model, ^{99m}Tc-3PRGD$_2$ tumor uptake decreased following treatment with bevacizumab. ^{99m}Tc-3PRGD$_2$SPECT/CT may be used as a non-invasive tool to evaluate the early biological effects of anti-angiogenic therapy.

Acknowledgements

This study was supported by the Research Fund of Science and Technology Department of Jilin Province (grant nos. 20150520154JH and 20160101064JC), the Foundation of National Health and Family Planning Commission of Jilin Province (grant nos. 2015Q020 and 2016Q038), the Department of Education of Jilin Province for Thirteen-Five Scientific Technique Research [grant no. (2016) 460], the Norman Bethune Program of Jilin University (grant no. 2015437) and Jilin University Funding Project for Young Teacher Cultivation Plan (grant no. 419080500365).

References

1. Rayson D, Vantyghem SA and Chambers AF: Angiogenesis as a target for breast cancer therapy. J Mammary Gland Biol Neoplasia 4: 415-423, 1999.
2. Ferrara N and Kerbel RS: Angiogenesis as a therapeutic target. Nature 438: 967-974, 2005.
3. Rodgers M, Soares M, Epstein D, Yang H, Fox D and Eastwood A: Bevacizumab in combination with a taxane for the first-line treatment of her2-negative metastatic breast cancer. Health Technol Assess 15 (Suppl 1): S1-S12, 2011.
4. Sheng J, Yang YP, Yang BJ, Zhao YY, Ma YX, Hong SD, Zhang YX, Zhao HY, Huang Y and Zhang L: Efficacy of addition of antiangiogenic agents to taxanes-containing chemotherapy in advanced nonsmall-cell lung cancer: A meta-analysis and systemic review. Medicine (Baltimore) 94: e1282, 2015.
5. Lee SM, BAAS P and Wakelee H: Anti-angiogenesis drugs in lung cancer. Respirology 15: 387-392, 2010.
6. Lange A, Prenzler A, Frank M, Golpon H, Welte T and von der Schulenburg JM: A systematic review of the cost-effectiveness of targeted therapies for metastatic non-small cell lung cancer (nsclc). BMC Pulm Med 14: 192, 2014.
7. Schreuder SM, Lensing R, Stoker J and Bipat S: Monitoring treatment response in patients undergoing chemoradiotherapy for locally advanced uterine cervical cancer by additional diffusion-weighted imaging: A systematic review. J Magn Reson Imaging 42: 572-594, 2015.
8. Lei L, Wang X and Chen Z: PET/CT imaging for monitoring recurrence and evaluating response to treatment in breast cancer. Adv Clin Exp Med 25: 377-382, 2016.
9. Ji B, Chen B, Wang T, Song Y, Chen M, Ji T, Wang X, Gao S and Ma Q: ^{99}mTc-3PRGD$_2$ SPECT to monitor early response to neoadjuvant chemotherapy in stage II and III breast cancer. Eur J Nucl Med Mol Imaging 42: 1362-1370, 2015.
10. Ma Q, Min K, Wang T, Chen B, Wen Q, Wang F, Ji T and Gao S: (99m)Tc-3PRGD 2 SPECT/CT predicts the outcome of advanced nonsquamous non-small cell lung cancer receiving chemoradiotherapy plus bevacizumab. Ann Nucl Med 29: 519-527, 2015
11. Jia B, Liu Z, Zhu Z, Shi J, Jin X, Zhao H, Li F, Liu S and Wang F: Blood clearance kinetics, biodistribution, and radiation dosimetry of a kit-formulated integrin αvβ3-selective radiotracer 99mTc-3PRGD2 in non-human primates. Mol Imaging Biol 13: 730-736, 2011.
12. Niu G and Chen X: Why integrin as a primary target for imaging and therapy. Theranostics 1: 30-47, 2011.
13. Wang L, Shi J, Kim YS, Zhai S, Jia B, Zhao H, Liu Z, Wang F, Chen X and Liu S: Improving tumor-targeting capability and pharmacokinetics of (99m)Tc-labeled cyclic RGD dimers with PEG(4) linkers. Mol Pharm 6: 231-245, 2009.
14. Zhou Y, Kim YS, Chakraborty S, Shi J, Gao H and Liu S: 99mTc-labeled cyclic RGD peptides for noninvasive monitoring of tumor integrin $\alpha_v\beta_3$ expression. Mol Imaging 10: 386-397, 2011.
15. Distler JH, Hirth A, Kurowska-Stolarska M, Gay RE, Gay S and Distler O: Angiogenic and angiostatic factors in the molecular control of angiogenesis. Q J Nucl Med 47: 149-161, 2003.
16. Wong CI, Koh TS, Soo R, Hartono S, Thng CH, McKeegan E, Yong WP, Chen CS, Lee SC, Wong J, *et al*: Phase I and biomarker study ofABT-869, a multiple receptor tyrosine kinase inhibitor, in patients with refractory solid malignancies. J Clin Oncol 27: 4718-4726, 2009.
17. Jiang F, Albert DH, Luo Y, Tapang P, Zhang K, Davidsen SK, Fox GB, Lesniewski R and McKeegan EM: ABT-869, a multi-targeted receptor tyrosine kinase inhibitor, reduces tumor microvascularity and improves vascular wall integrity in preclinical tumor models. J Pharmacol Exp Ther 338: 134-142, 2011.
18. Tannir NM, Wong YN, Kollmannsberger CK, Ernstoff MS, Perry DJ, Appleman LJ, Posadas EM, Cho D, Choueiri TK, Coates A, *et al*: Phase 2 trial of linifanib (ABT-869) in patients with advanced renal cell cancer after sunitinib failure. Eur J Cancer 47: 2706-2714, 2011.
19. Gullino PM: Angiogenesis and neoplasia. N Engl J Med 305: 884-885, 1981.
20. Koukourakis MI, Giatromanolaki A, Sivridis E and Fezoulidis I: Cancer vascularization: Implications in radiotherapy? Int J Radiat Oncol Biol Phys 48: 545-553, 2000.
21. Morrison MS, Ricketts SA, Barnett J, Cuthbertson A, Tessier J and Wedge SR: Use of a novel Arg-Gly-Asp radioligand, 18F-AH111585, to determine changes in tumor vascularity after antitumor therapy. J Nucl Med 50: 116-122, 2009.
22. Battle MR, Goggi JL, Allen L, Barnett J and Morrison MS: Monitoring tumor response to antiangiogenic sunitinib therapy with 18F-fluciclatide, an 18F-labeled αVbeta3-integrin and αVbeta5-integrin imaging agent. J Nucl Med 52: 424-430, 2011.
23. Sun X, Yan Y, Liu S, Cao Q, Yang M, Neamati N, Shen B, Niu G and Chen X: 18F-FPPRGD2 and 18F-FDG PET of response to Abraxane therapy. J Nucl Med 52: 140-146, 2011.
24. Zhou Y, Kim YS, Lu X and Liu S: Evaluation of 99mTc-labeled cyclic RGD dimers: Impact of cyclic RGD peptides and 99mTc chelates on biological properties. Bioconjug Chem 23: 586-595, 2012.